THE DEVELOPMENT OF THREE-DIMENSIONAL TURBULENT SURFACE JETS

Tim J Craft, Jasper W Kidger and Brian E Launder
Mechanical Engineering Department, UMIST,
PO Box 88, Manchester, UK

ABSTRACT

The paper explores the computation of a turbulent liquid jet discharged at the free surface of an expanse of the same fluid at rest. The turbulent stress field has been modelled by second-moment closure wherein transport equations are solved for each of the Reynolds stresses. The model of the pressure-strain correlation is especially influential on the flow's development. Two alternatives are explored: the basic return-to-isotropy model with free-surface reflection terms and the newer two-component-limit (TCL) model developed at UMIST over the past decade.

The computations show that the TCL model is indeed much more successful than the simpler alternative for this flow. Experimental data are limited to the near-field but our calculations suggest that to reach the asymptotic rates of spread requires well over 100 discharge diameters of development. The exceptional distance is due to the gradual growth of streamwise vorticity driven by the strongly anisotropic Reynolds stress field acting in the jet's cross-section.

1. INTRODUCTION

The three-dimensional surface jet, like the more extensively studied three-dimensional wall jet, is a flow dominated in the far field by the creation of appreciable streamwise vorticity and the interaction of this vorticity source with the primary flow. While, in principle, if the surroundings are at rest, the flow should evolve to a self-similar form, the mutual interaction between the primary shear and the secondary flow means that a development length of well over 100 initial diameters is needed to reach the asymptotic state.

These assertions are based partly on indicators from our companion study on wall jets (Craft & Launder, 1999) and partly on numerical results obtained in the present research. They could not, it is important to note, be inferred from experimental measurements of surface jets since these explorations have extended only some 40 initial diameters from discharge, Rajaratnam & Humphries (1984), Anthony & Willmarth (1992), at which point it was assumed that the flow had reached, or was close to, the self-preserving state.

The question of the asymptotic character of surface jets is of considerable environmental interest. For example, in water-cooled power stations, it is important to be able to provide an accurate assessment of the impact of the warm water discharged into a lake or river, which implies knowing or being able to compute mixing rates accurately.

The writers' study on wall jets (Craft & Launder, 1999) has mainly considered the self-similar behaviour. In the present exploration, however, because experimental documentation covers only the initial stages of development, we have focused on the developing flow regime by way of a 3D solver. The wall jet computations had compared eddy-viscosity and second-moment computations but the former were shown to be incapable of creating the substantial streamwise vorticity that drives the flow. Accordingly, here computations are limited to the case where the turbulent stresses are approximated by second-moment closure. In the present contribution attention is limited to the isothermal case. The non-isothermal behaviour, including the important influence of buoyancy will be considered in a future paper.

2. THE NUMERICAL MODEL

2.1 Numerical Aspects

The full Reynolds equations (rather than a boundary-layer truncation) were solved in segments on an expanding mesh as indicated in Fig 1 together with the corresponding stress transport and dissipation equations noted in Section 2.2. The STREAM-3D solver, developed and made available to us in software form by Lien & Leschziner (1994), was employed. This is a structured, non-orthogonal solver with a collocated mesh. In the present application, the jet cross-

section is mapped with a Cartesian grid while, in the stream direction (x), the grid expands as needed in the vertical (y) and horizontal (z) directions to cover the domain influencing the jet development.

The weak effects of downstream events on the upstream flow enabled us to tackle the flow development by successively considering a small block of the flow domain, starting at the point of discharge of the jet and applying zero gradient conditions on the out-flowing fluid. When this block had converged, one proceeded to Block 2 beginning the computation well inside the downstream extent of Block 1 with entry conditions determined from the solution of the first block. This "block marching" approach was repeated at further downstream positions. For each block a 50 (streamwise) x 65 x 65 expanding mesh was adopted. Entrainment to the domain on constant -y or -z surfaces is required to be normal to the boundaries. Craft & Launder (1999) have verified that this is a satisfactory practice though it probably requires a larger solution domain than if zero vorticity at the entrainment boundaries had been prescribed. This latter practice was tried but unfortunately did not lead to converged solutions.

2.2 The Turbulence Models Considered

As noted, only second-moment closures are considered where transport equations are solved for the six Reynolds stresses, $\overline{u_i u_j}$, and the energy dissipation rate, ε.

The equations solved may thus be written symbolically as:

$$\frac{D\overline{u_i u_j}}{Dt} = P_{ij} + \phi_{ij} + d_{ij} - \varepsilon_{ij} \qquad (1)$$

$$\frac{D\varepsilon}{Dt} = P_\varepsilon + d_\varepsilon - \varepsilon_\varepsilon \qquad (2)$$

In the above P_{ij}, ϕ_{ij}, ε_{ij} and d_{ij} are respectively the generative, redistributive, dissipative and diffusive rates of $\overline{u_i u_j}$. The first of these is handled without approximation:

$$P_{ij} \equiv -\left(\overline{u_i u_k} \frac{\partial U_j}{\partial x_k} + \overline{u_j u_k} \frac{\partial U_i}{\partial x_k} \right) \qquad (3)$$

The most crucial element to approximate for the present flow is believed to be the non-dispersive fluctuating pressure interaction, ϕ_{ij} comprising mean strain and purely turbulence effects. In the case of the *Basic Model*, 'wall-reflection' effects are applied to the free surface in accord with the conclusions of Reece (1977) and McGuirk & Papadimitriou (1985) that this practice led to clearly superior predictions. The particular 'wall-reflection' correction employed is that proposed by Craft & Launder (1992) to accommodate flow impinging on as well as parallel to a wall. (Because of the strong vertical entrainment the present flow has similarities to both these flow types.) Thus :

$$\phi_{ij} = -c_1 \frac{\varepsilon}{k}\left(\overline{u_i u_j} - \frac{2}{3}\delta_{ij} k \right) - c_2 \left(P_{ij} - \frac{1}{3}\delta_{ij} P_{kk} \right) + \phi_{ij}^{wr} \qquad (4)$$

where, in the interests of space, the wall-reflection contribution is not detailed.

The second scheme is the Two-Component-Limit (TCL) model developed at UMIST over the past dozen years from a strategy proposed by Lumley (1978) The most relevant feature is that, even for flow near walls, it employs *no* wall reflection, Launder & Li (1994), Iacovides et al (1996). The particular form used here is from Craft (1998) though, because the present flow contains no viscous sublayer and the motion is predominantly parallel to the surface, the somewhat simpler version of Launder & Li with constant coefficients would have given essentially the same results.

$$\begin{aligned}
\phi_{ij} &= \phi_{ij1} + \phi_{ij2} \\
\phi_{ij1} &= -C_1 \varepsilon \left[a_{ij} + C_1' \left(a_{ik} a_{jk} - \frac{1}{3} A_2 \delta_{ij} \right) \right] - A^{0.5} \varepsilon a_{ij} \\
\phi_{ij2} &= -0.6 \left(P_{ij} - \frac{1}{3}\delta_{ij} P_{kk} \right) + 0.3 \varepsilon a_{ij} \left(P_{kk} / \varepsilon \right) \\
&\quad - 0.2 \left[\frac{\overline{u_k u_j} \cdot \overline{u_l u_i}}{k} \left(\frac{\partial U_k}{\partial x_l} + \frac{\partial U_l}{\partial x_k} \right) - \frac{u_l u_k}{k} \left(\overline{u_i u_k} \frac{\partial U_j}{\partial x_l} + \overline{u_j u_k} \frac{\partial U_i}{\partial x_l} \right) \right] \\
&\quad - C_2 \left[A_2 \left(P_{ij} - D_{ij} \right) + 3 a_{mi} a_{nj} \left(P_{mn} - D_{mn} \right) \right] \\
&\quad + C_2' \left\{ \begin{array}{l}
\left(\frac{7}{15} - \frac{A_2}{4} \right) \left(P_{ij} - \frac{1}{3}\delta_{ij} P_{kk} \right) - 0.05 a_{ij} a_{lk} P_{kl} \\
+ 0.1 \varepsilon \left[a_{ij} - \frac{1}{2} \left(a_{ik} a_{kj} - \frac{1}{3}\delta_{ij} A_2 \right) \right] \left(P_{kk} / \varepsilon \right) \\
+ 0.1 \left[\left(\frac{\overline{u_i u_m}}{k} P_{mj} + \frac{\overline{u_j u_m}}{k} P_{mi} \right) - \frac{2}{3}\delta_{ij} \frac{\overline{u_l u_m}}{k} P_{ml} \right] \\
+ 0.2 \frac{\overline{u_k u_j} \cdot \overline{u_l u_i}}{k^2} \left(D_{lk} - P_{lk} \right) \\
+ 0.1 \left[\frac{\overline{u_k u_j} \cdot \overline{u_l u_i}}{k^2} - \frac{1}{3}\delta_{ij} \frac{\overline{u_l u_m} \cdot \overline{u_k u_m}}{k^2} \right] \\
\quad \times \left[6 D_{lk} + 13 k \left(\frac{\partial U_l}{\partial x_k} + \frac{\partial U_k}{\partial x_l} \right) \right]
\end{array} \right\}
\end{aligned} \qquad (5)$$

In the above, the following standard notation is adopted :

$$a_{ij} \equiv \frac{\overline{u_i u_j}}{k} - \frac{2}{3}\delta_{ij} \qquad A_2 \equiv a_{ij} a_{ji} \qquad A_3 \equiv a_{ij} a_{jk} a_{ki}$$

$$A \equiv 1 - 9/8 \left(A_2 - A_3 \right) \qquad A_{2d} \equiv min\left(A_2, 0.5 \right)$$

$$D_{ij} \equiv -\left[\overline{u_i u_k}\frac{\partial U_k}{\partial x_j} + \overline{u_j u_k}\frac{\partial U_k}{\partial x_i}\right]$$

$$S \equiv \frac{k}{\varepsilon}\left(\frac{1}{2}S_{ij}S_{ij}\right)^{1/2} \qquad S_{ij} \equiv \frac{\partial U_i}{\partial x_j} + \frac{\partial U_j}{\partial x_i}$$

$$S_1 \equiv S_{ij}S_{jk}S_{ki}/(S_{ln}S_{ln})^{3/2}$$

$$\Omega \equiv \frac{k}{\varepsilon}\left(\frac{1}{2}\Omega_{ij}\Omega_{ij}\right)^{1/2} \qquad \Omega_{ij} \equiv \frac{\partial U_i}{\partial x_j} - \frac{\partial U_j}{\partial x_i}$$

And the empirical coefficients are assigned as Craft (1998):

$$C_1 = 3.1 f_A A_{2d} \qquad C_1' = 1.1$$

$$C_2 = min[0.55, 3.2A/(1+S)]$$

$$C_2' = min(0.6, A) + 2(S-\Omega)/(3+S+\Omega) - 1.5S_1$$

$$f_A = \begin{cases} A\left(\dfrac{0.05}{0.7}\right)^{1/2} & for\ A < 0.05 \\ \dfrac{A}{(0.7)^{1/2}} & 0.05 < A < 0.7 \\ A & A > 0.7 \end{cases} \qquad (6)$$

Two distinct approximations are likewise made for ε_{ij}. With the Basic Model of ϕ_{ij} , it is simply assumed that the flow remains locally isotropic :

$$\varepsilon_{ij} = \frac{2}{3}\delta_{ij}\varepsilon \qquad (7)$$

Although it is improbable that the dissipation precisely maintains isotropy, this certainly gives a better estimate than the usual alternative $\varepsilon_{ij} = \dfrac{\overline{u_i u_j}\varepsilon}{k}$ (which would imply zero dissipation of the vertical normal stress at the free surface). With the more elaborate TCL model of ϕ_{ij} , we likewise adopt a model for ε_{ij} which satisfies the two-component limit (Craft & Launder, 1996) :

$$\varepsilon_{ij} = (1-A)\left(\varepsilon_{ij}' + \varepsilon_{ij}''\right)/D + \frac{2}{3}A\delta_{ij}\varepsilon \qquad (8)$$

where :

$$\varepsilon_{ij}' = \frac{\varepsilon}{k}\overline{u_i u_j} + 2\nu\frac{\overline{u_l u_n}}{k}\frac{\partial\sqrt{k}}{\partial x_l}\frac{\partial\sqrt{k}}{\partial x_n}\delta_{ij} + 2\nu\frac{\overline{u_l u_i}}{k}\frac{\partial\sqrt{k}}{\partial x_j}\frac{\partial\sqrt{k}}{\partial x_l} + 2\nu\frac{\overline{u_l u_j}}{k}\frac{\partial\sqrt{k}}{\partial x_i}\frac{\partial\sqrt{k}}{\partial x_l}$$

$$\varepsilon_{ij}'' = \varepsilon\left[2\frac{\overline{u_l u_k}}{k}d_l^a d_k^a \delta_{ij} - \frac{\overline{u_l u_i}}{k}d_l^a d_j^a - \frac{\overline{u_l u_j}}{k}d_l^a d_i^a\right](1-A)$$

$$D = (\varepsilon_{kk}' + \varepsilon_{kk}'')/2\varepsilon \qquad d_i^a = \frac{N_i}{0.5 + (N_k N_k)^{0.5}}$$

$$N_i = \frac{\partial}{\partial x_i}\left(\frac{k^{3/2}A^{1/2}}{\varepsilon}\right) \qquad (9)$$

Equation (2) for the dissipation rate nominally takes the same form for both models. The generalized gradient diffusion hypothesis is adopted for both models:

$$d_\varepsilon = \frac{\partial}{\partial x_k}\left[\left(c_\varepsilon\frac{k}{\varepsilon}\overline{u_k u_l} + \nu\delta_{kl}\right)\frac{\partial\varepsilon}{\partial x_l}\right] \qquad (10)$$

while for the source and sink terms the usual representation is retained:

$$P_\varepsilon = c_{\varepsilon 1}\frac{P_{kk}\varepsilon}{2k} \qquad \varepsilon_\varepsilon = c_{\varepsilon 2}\frac{\varepsilon^2}{k} \qquad (11)$$

There is, however, a significant difference in the choice of the empirical coefficients. The Basic Model adopts the constant values:

$$c_{\varepsilon 1} = 1.44 \qquad c_{\varepsilon 2} = 1.92 \qquad (12)$$

The TCL model instead adopts:

$$c_{\varepsilon 1} = 1.00 \qquad c_{\varepsilon 2} = 1.92/\left(1 + 0.7A_2^{0.5}A_{25}\right) \qquad (13)$$

where $A_{25} \equiv$ max (A,0.25); $A \equiv 1 - \dfrac{9}{8}(A_2 - A_3)$ (Lumley's (1978) "flatness" parameter); and $A_3 \equiv a_{ij}a_{jk}a_{ki}$.

It perhaps needs to be underlined that the particular choice of coefficients has been set several years ago by reference to quite different flows to that considered here.

2.3 Boundary Conditions

Along the vertical symmetry plane, z = 0, the usual symmetry plane boundary conditions are applied while, at the outer edges, the secondary velocities were set to a zero gradient. For stability, the turbulent quantities were set to a zero gradient along the outer boundaries if there was mass outflow, or set to zero if there was inflow.

The most influential conditions are those applied at inlet and at the free surface. At inlet, the jet is assumed to have a boundary layer of approximately 30% of the jet radius (unfortunately, the experimental studies do not describe the profile of the jet at inlet). At the free surface the mean velocity gradient parallel to the free surface was set to zero while the vertical velocity was itself zeroed. Correspondingly, the surface shear-stresses and $\overline{v^2}$ were assigned zero values while the vertical gradients of the other two normal stresses were set to zero. The question of the

most appropriate free-surface condition for ε is not entirely resolved. Here, the value of ε at the near-surface node is prescribed from a length scale :

$$\varepsilon = \frac{C_\mu^{0.75} k^{1.5}}{\kappa y} \tag{14}$$

with C_μ=0.09 , κ=0.4187 , and y is the distance of the node from the free surface.

3. PRESENTATION AND DISCUSSION OF RESULTS

The computed development of the surface jet is compared with the experimental data of Rajaratnam & Humphries (1984) in Figures 2 and 3; Figure 2 includes computational results for the Basic Model, Figure 3 the corresponding comparisons for the TCL model. These figures show profiles of streamwise velocity on the symmetry plane (z = 0) and on the horizontal plane passing through the position of maximum velocity (for a given x). From Figure 2 it is evident that the Basic Model fails very seriously to provide an account of the jet development in reasonable accord with experiment. There is a much too rapid horizontal spreading leading to a decay of maximum velocity that is much too fast despite the fact that the vertical spreading rate is appreciably too low.

The corresponding development with the TCL model, Figure 3, is in much closer agreement with experiment. Nevertheless, one may note from Fig 3b that the velocity decay rate is still somewhat too large (certainly for x/d greater than 12) while beyond x/d = 7.4 the computed near-surface velocity profile, Fig 3a, does not exhibit the dip in velocity as the free surface is approached that is evident in the experiments. This observed dip in velocity is evidently due to convective transport of low momentum fluid from below (i.e. from regions where y is large); that is, it is associated with the computed secondary flow which, we show below, is in turn driven by the anisotropy of the Reynolds stresses in the cross-section of the jet (the y-z plane). Now, the fact that the computed horizontal spreading rate is somewhat too large implies a too large secondary flow while - on the contrary - the absence of a dip in the $U(y)$ profile near the free surface suggests a secondary flow that is too small! The explanation of this paradox is perhaps that the boundary condition imposed on ε leads to a seriously incorrect variation of $\overline{v^2}-\overline{w^2}$ very near the free surface and thus to an underestimate of the vorticity source giving a too low W velocity near the free surface.

The spreading behaviour of the surface jet is conveniently summarised in Fig 4 which shows the progressive growth of the half-widths with distance downstream. This figure brings out the very clear superiority of the TCL model in reproducing the actual growth pattern of the jet.

Although no measured values of secondary flow were obtained, it is instructive to note the variation of the maximum secondary velocities. It is found that the vertical velocity (V) remains roughly 5% of the axial velocity (U) for both the Basic and TCL models. However, the lateral (W) velocity (Fig 5) increases with distance downstream, and as suggested by the previous figures, the Basic model produces a much stronger lateral (W) velocity.

The build-up of the secondary velocity towards the free surface from below and parallel to the free surface, away from the symmetry plane, is indicative of the creation of appreciable streamwise vorticity in the jet. It is of interest to identify the source of this vorticity. The axial vorticity (Ω_x) equation neglecting viscous terms may be written:

$$\frac{D\Omega_x}{Dt} = \underbrace{\Omega_x \frac{\partial U}{\partial x}}_{A} + \underbrace{\Omega_y \frac{\partial U}{\partial y} \Omega_z \frac{\partial U}{\partial z}}_{B} + \underbrace{\frac{\partial^2}{\partial y \partial z}\left[\overline{w^2} - \overline{v^2}\right]}_{C} + \underbrace{\frac{\partial^2 \overline{vw}}{\partial y^2} - \frac{\partial^2 \overline{vw}}{\partial z^2}}_{D} \tag{15}$$

where $\Omega_x \equiv \left(\frac{\partial V}{\partial z} - \frac{\partial W}{\partial y}\right)$, etc.

The variation of terms A - D over the cross section of the wall jet at x/d = 20 is shown in contour form in Figs 6a-6c. Two things are evident: firstly that the vortex line bending terms (B) are less important than the axial stretching (or, in this case, squashing) of vortex lines (terms A); secondly, that both these mean field sources of vorticity are small compared with that associated with spatial gradients of the Reynolds stresses (C+D).

4. CONCLUSIONS

The following principal conclusions may be drawn from this computational study of developing free-surface jets.

i) While experimental data of surface jets extend to 40 diameters downstream, this is by no means far enough to reach full development. Indeed, our separate study of fully-developed surface jets (Craft et al, 1999) indicates that the asymptotic horizontal spread is some 60% greater than that at 40d.

ii) The enhanced spreading is due to the strong streamwise vorticity created by spatial variations in the anisotropy of the Reynolds stress field over the jet cross section. Even at 20 diameters downstream, this source far outweighs that associated with vortex line bending.

iii) A second-moment closure based on Lumley's (1978) two-component-limit provides a generally satisfactory mimicking of the flow development even though the detailed form of the closure has been fixed by earlier studies of quite different flows.

iv) Certain anomalies in the predicted axial velocity close to the free surface suggest that some reconsideration of the appropriate surface boundary condition for ε is needed.

ACKNOWLEDGEMENTS

The basic STREAM software was made available for this study by Dr F S Lien and Professor M A Leschziner. The Royal Society have provided a University Research Fellowship for T J Craft while J W Kidger has been supported by an EPSRC studentship. Authors' names appear alphabetically.

REFERENCES

Anthony D.G., Willmarth W.W., 1992, "Turbulence Measurements in a Round Jet Beneath a Free Surface", *J.Fluid Mechanics, **243**,* pp699-720

Craft T.J., 1998, "Developments in a Low-Reynolds-Number Second-Moment Closure and its Application to Separating and Reattaching Flows", *Int. J. Heat and Fluid Flow, **19**,* pp541-548

Craft T.J., Kidger J.W., Launder B.E., 1999, "Three Dimensional Modelling of Turbulent Free-Surface Jets", *4th Int. Sym. on Engineering Turbulence Modelling and Measurements, Corsica, France.*

Craft T.J., Launder B.E., 1992, "New Wall-Reflection Model Applied to the Turbulent Impinging Jet", *AIAA Journal, **30**,* pp2970-2972

Craft T.J., Launder B.E., 1996, "A Reynolds stress closure designed for complex geometries", *Int. J. Heat and Fluid Flow, **17**,* pp245-254

Craft T.J., Launder B.E., 1999, "The Self-Preserving, Three-Dimensional Turbulent Wall Jet", *Submitted for Publication*

Iacovides H., Launder B.E., Li H.-Y., 1996, "Application of a Reflection-Free DSM to Turbulent Flow and Heat Transfer in a Square-Sectioned U-Bend", *Experimental Thermal and Fluid Science, **13**,* pp419-429

Launder B.E., Li S.-P., 1994, "On the Elimination of Wall-Topography Parameters from Second-Moment Closure", *Phys. Fluids. **6-2***, pp 999-1006

Lien F.-S., Leschziner M.A., 1994, "A general non-orthogonal finite-volume algorithm for turbulent flow at all speeds incorporating second-moment turbulence-transport closure", *Comp. Meth. Appl. Mech. Eng., **114**,* pp123-167

Lumley J.L., 1978, "Computational Modelling of Turbulent Flows" *Adv. Appl. Mech. **18***, p123

McGuirk J.J., Papadimitriou C., 1985, "Buoyant Surface Layers Under Fully Entraining and Internal Hydraulic Jump Conditions" *5th Sym. on Turbulent Shear Flows, Cornell University, 1985*

Rajaratnam N., Humphries, J.A., 1984, "Turbulent Non-Buoyant Surface Jets", *J. Hydraulic Research, **22**,* pp103-115

Reece G.J., 1977, "A generalised Reynolds stress model of turbulence", PhD thesis, Faculty of Engineering, University of London.

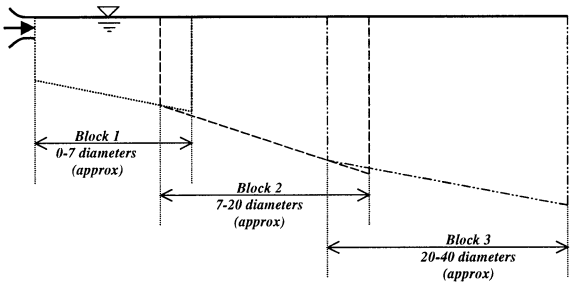

Figure 1. The solution domain involving overlapping downstream blocks

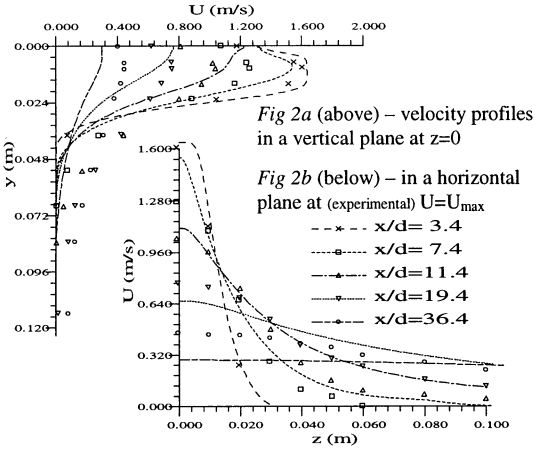

Figure 2. Streamwise Velocity Profiles computed with the 'Basic' Model. Data points from laboratory work of Rajaratnam & Humphries (1984)

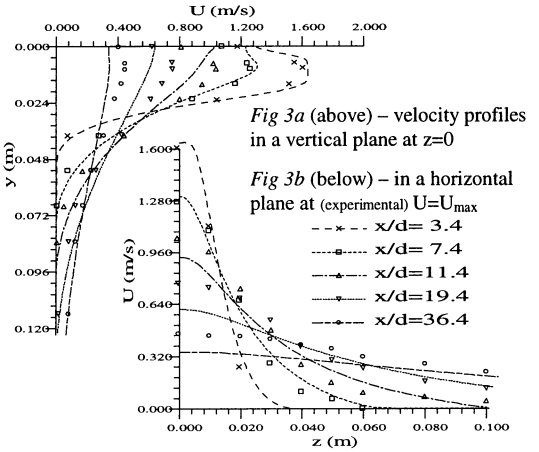

Figure 3. Streamwise Velocity Profiles computed with the 'TCL' Model. Data points from laboratory work of Rajaratnam & Humphries (1984)

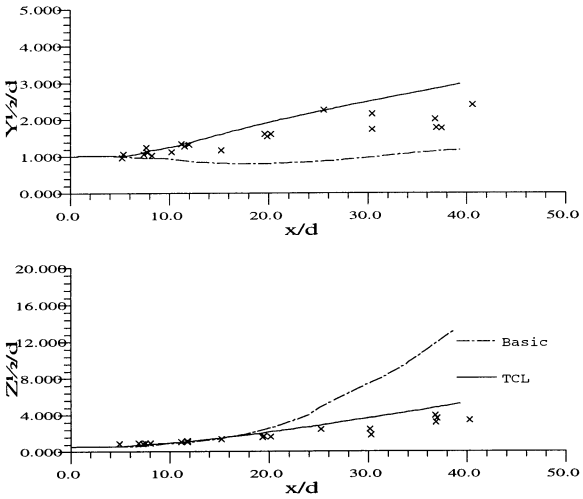

Figure 4. Vertical (top) and horizontal (lower) variations in jet half-width for 'Basic' and 'TCL' models, compared with data of Rajaratnam & Humphries (1984)

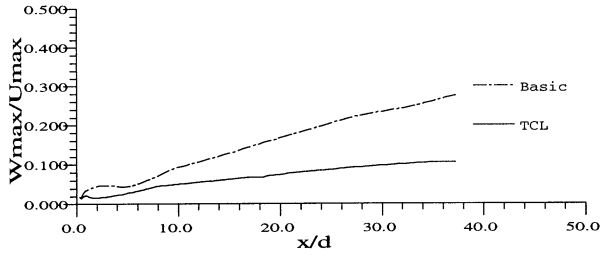

Figure 5. Magnitude of lateral velocity with distance downstream for 'Basic' and 'TCL' models.

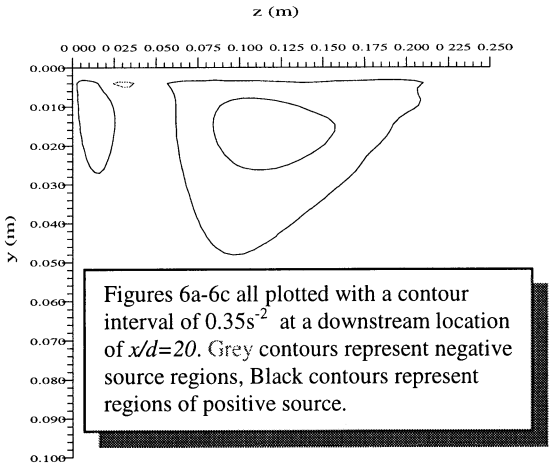

Figure 6a Vorticity budget – Term 'A' in equation 15

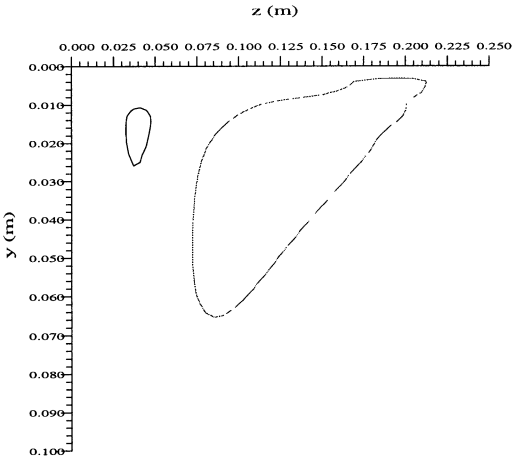

Figure 6b Vorticity budget – Term 'B' in equation 15

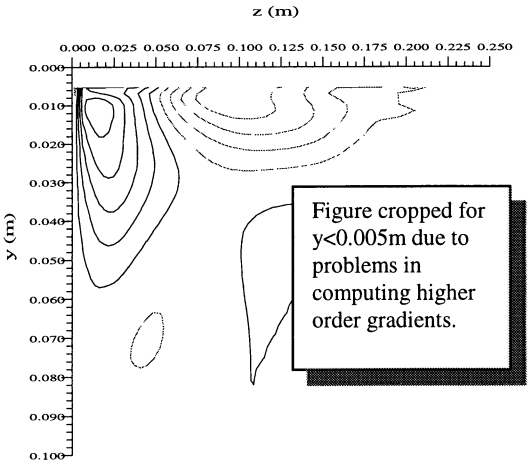

Figure 6c Vorticity budget – Terms 'C+D' in equation 15